Title	Low-Z shore of the “island of inversion” and the reduced neutron magicity toward ²⁸O
Author(s)	Doornenbal, P; Scheit, H; Takeuchi, S; Utsuno, Y; Aoi, N; Li, K; Matsushita, M; Steppenbeck, D; Wang, H; Baba, H; Ideguchi, E; Kobayashi, N; Kondo, Y; Lee, HCJ; Michimasa, S; Motobayashi, T; Otsuka, T; Sakurai, H; Takechi, M; Togano, Y; Yoneda, K
Citation	Physical Review C: covering nuclear physics, 2017, v. 95 n. 4, p. 041301(R):1-5
Issued Date	2017
URL	http://hdl.handle.net/10722/241629
Rights	Physical Review C: covering nuclear physics. Copyright © American Physical Society.; This work is licensed under a Creative Commons Attribution-NonCommercial-NoDerivatives 4.0 International License.

PHYSICAL REVIEW C **95**, 041301(R) (2017)

Low-Z shore of the "island of inversion" and the reduced neutron magicity toward ^{28}O

P. Doornenbal,[1,*] H. Scheit,[1,2,†] S. Takeuchi (武内 聡),[1,‡] Y. Utsuno (宇都野 穣),[3] N. Aoi (青井 考),[1,§] K. Li (李 闊昂),[1,2] M. Matsushita (松下 昌史),[1,4,‖] D. Steppenbeck,[1] H. Wang (王 赫),[1,2] H. Baba (馬場 秀忠),[1] E. Ideguchi (井手口　栄治),[5,§] N. Kobayashi (小林 信之),[6,§] Y. Kondo (近藤 洋介),[6] J. Lee (李曉菁),[1,¶] S. Michimasa (道正　新一郎),[5] T. Motobayashi (本林 透),[1] T. Otsuka (大塚 孝治),[5,7] H. Sakurai (櫻井 博儀),[1] M. Takechi (武智 麻耶),[1,#] Y. Togano (栂野 泰宏),[1,‡] and K. Yoneda (米田健一郎)[1]

[1]*RIKEN Nishina Center, Wako, Saitama 351-0198, Japan*

[2]*Peking University, Beijing 100871, People's Republic of China*

[3]*Advanced Science Research Center, Japan Atomic Energy Agency, Tokai, Ibaraki 319-1195, Japan*

[4]*Department of Physics, Rikkyo University, Toshima, Tokyo 172-8501, Japan*

[5]*Center for Nuclear Study, University of Tokyo, RIKEN Campus, Wako, Saitama 351-0198, Japan*

[6]*Department of Physics, Tokyo Institute of Technology, Meguro, Tokyo 152-8551, Japan*

[7]*Department of Physics, University of Tokyo, Bunkyo, Tokyo 113-0033, Japan*

(Received 11 February 2015; revised manuscript received 20 February 2017; published 13 April 2017)

The two odd-even fluorine isotopes ^{27,29}F were studied via in-beam γ-ray spectroscopy at the RIKEN Radioactive Isotope Beam Factory. A secondary beam of ^{30}Ne was used to induce one-proton and one-proton–two-neutron removal reactions on carbon and polyethylene targets at midtarget energies of 228 MeV/u. Excited states were observed at 915(12) keV for ^{27}F and at 1080(18) keV for ^{29}F. Both were assigned a $1/2^+_1$ spin and parity. The low transition energy for ^{29}F largely disagrees with shell model predictions restricted to the *sd* model space. Calculations using effective interactions that include the neutron *pf* shell indicate that the $N = 20$ gap is quenched for ^{29}F, thus extending the "island of inversion" to isotopes with proton number $Z = 9$. Variations of the $N = 20$ gap further reveal a strong correlation to the $1/2^+_1$ level energy in ^{29}F and suggest a persistent reduced neutron gap for ^{28}O.

DOI: 10.1103/PhysRevC.95.041301

The properties of nuclei far away from the valley of β stability are essential for our comprehension of the underlying forces between nucleons. When located inside an atomic nucleus, the nucleons, i.e., the protons and neutrons, are arranged to form shells by independent particle filling in a mean potential representing contributions from all nucleons. The proton and neutron numbers necessary to complete the filling of the shells, the "magic" numbers, were first correctly reproduced theoretically by introducing a large spin-orbit force and constitute the cornerstone of the nuclear shell model [1,2]. With knowledge of nuclear structure extending closer to the driplines, it has become evident that magic numbers are not constant across the Segré (N,Z) chart of nuclei [3]. Examples of new neutron magic numbers have been reported in neutron-rich oxygen ($N = 16$) and calcium ($N = 32,34$) isotopes, established by spectroscopy of a high first excited 2^+ state [4–6], as well as a large two-neutron shell gap for ^{52}Ca [7]. Of interest in this context is the structure of nuclei adjacent to doubly magic nuclei for which both proton and neutron shells are filled completely. They can be regarded as a single valence nucleon in addition to an inert core, thereby diminishing the many-body problem. This results in simplified structures and gives access to the location of the single-particle energies.

Composed of the traditional magic numbers $Z = 8$ and $N = 20$, ^{28}O is an anticipated doubly magic nucleus. This region of the nuclear chart features an intriguing interplay between three-nucleon [8] and tensor forces [9,10]. It has been shown that the former can account for the anomalous location of the dripline for oxygen isotopes [11–14], while the latter generates the new magic number $N = 16$ for ^{24}O [5,9,15]. Heavier oxygen isotopes are unbound against neutron emission [16,17] and, therefore, cannot be accessed directly. Adding only a single proton to the nucleus, i.e., going from oxygen to fluorine isotopes, provides sufficient additional binding energy to shift the dripline by six neutrons to ^{31}F [17]. It has been predicted that the $N = 20$ shell gap quenching observed for heavier isotopes around ^{32}Mg [18,19] extends to the fluorine isotopes [20] and merges for neutron-rich neon, sodium, and magnesium isotopes with the $N = 28$ shell gap quenching [21]. Indeed, low 2^+_1 excitation energies are found in this region of the Segré chart, commonly referred to as "island of inversion" [22], up to $N = 26$ for magnesium isotopes [18,23–25] and up to $N = 22$ for neon isotopes [26,27], while the odd-Z sodium isotopes feature rotational character [28]. Schematically, the ground states of island of inversion nuclei

*pieter@ribf.riken.jp

†Present address: Institut für Kernphysik, Technische Universität Darmstadt, Germany.

‡Present address: Department of Physics, Tokyo Institute of Technology, Japan.

§Present address: Research Center for Nuclear Physics, Osaka University, Japan.

‖Present address: Center for Nuclear Study, University of Tokyo, Japan.

¶Present address: Department of Physics, The University of Hong Kong, Hong Kong.

#Present address: Graduate School of Science and Technology, Niigata University, Japan.

are dominated by $\nu(sd)^{-2}(fp)^2(2\hbar\omega)$ configurations; owing to a reduced $N = 20$ gap the fp shell is occupied by two more neutrons than expected from a normal single-particle filling [22,29].

Little is known about the properties of the fluorine isotopes at the neutron dripline. A measurement of the unbound isotope ^{28}F pointed out that fp shell intruder components may be small in its ground-state structure [30], while a mass measurement of ^{29}F revealed no drastic drop in the two-neutron separation energy [31]. A precedent experiment reported on two transitions in ^{27}F at energies of 504(15) and 777(19) keV [32], but so far no γ-ray spectroscopic information exists for ^{29}F. In the present work, the two fluorine isotopes ^{27,29}F were studied following one-proton–two-neutron ($1p2n$) and one-proton ($1p$) removal reactions of an exotic ^{30}Ne beam at 228 MeV/u. Their structures bear crucial information on the magicitiy of ^{28}O and the "southern" boundaries of the island of inversion.

The experiment was carried out at the Radioactive Isotope Beam Factory, operated by the RIKEN Nishina Center and the Center for Nuclear Study of the University of Tokyo. After striking a ^{48}Ca primary beam of average intensity 80-particle nA and an energy of 345 MeV/u on a 2.8 g/cm^2 rotating beryllium production target, secondary cocktail beams containing mainly ^{30}Ne and ^{31}Na isotopes were selected in the first stage of the BigRIPS fragment separator [33]. Beam purification was achieved via the $B\rho$-ΔE-$B\rho$ method by applying two magnetic rigidity ($B\rho$) selections with a 10-mm-thick Al wedge-shaped degrader for the energy loss (ΔE) placed in-between the bending magnets. The momentum acceptance was set to the maximum value of 6%. Isotopes transported through the second stage of BigRIPS were identified with the $B\rho$-ΔE-TOF method by measuring their magnetic rigidities at the dispersive focal point, their times-of-flight (TOF) with two thin plastic scintillators and their energy losses in an ionization chamber. The secondary beam rate was 440 particles per second for ^{30}Ne. Details on the particle identification procedure with BigRIPS are described in Ref. [34]. The secondary beams were directed onto carbon and polyethylene targets with thicknesses of 2.54 and 2.13 g/cm^2, respectively, placed in front of the spectrometer ZeroDegree [33]. Due to the limited momentum acceptance of ≈8%, ZeroDegree was individually tuned for the ^{27,29}F reaction residues. Particles passing ZeroDegree were also identified with the $B\rho$-ΔE-TOF method. All fragments were unambiguously identified with BigRIPS and ZeroDegree, as shown in Fig. 1, which indicates the particle identification plot for ZeroDegree optimized for the transmission of ^{29}F.

γ rays emitted in flight following nucleon removal reactions were detected with the DALI2 spectrometer [35], an array composed of 186 large-volume NaI(Tl) crystals. DALI2 covered inclination angles from 18° to 147° in the laboratory system. Stationary sources of ^{60}Co, ^{88}Y, and ^{137}Cs were used for energy calibration and to determine the spectrometer's efficiency and matched simulations employing the GEANT4 software framework [36] with a relative error of ±6%. At midtarget, the average energy of the ^{30}Ne fragments was 228 MeV/u ($\beta \sim 0.596$). Thus, the γ-ray detection was subject to a large Doppler shift and broadening, leading to an anticipated energy resolution of 10% (FWHM) for γ rays of 1 MeV. Figure 2 displays the Doppler corrected γ-ray spectra in

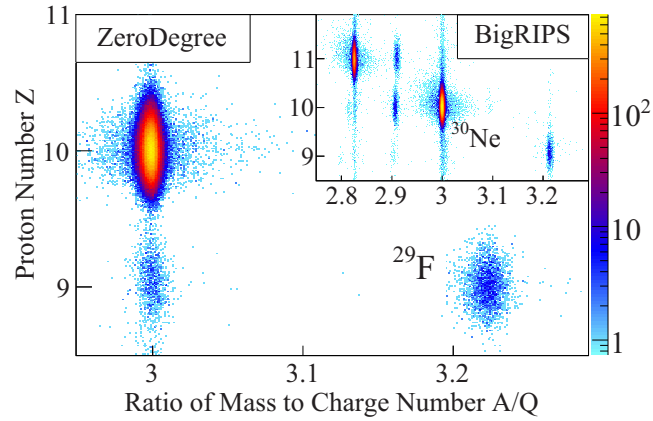

FIG. 1. Particle identification plot behind the secondary target with ^{30}Ne selected in BigRIPS and ZeroDegree tuned for ^{29}F. Secondary beams identified in BigRIPS are shown in the inset.

coincidence with the $1p2n$ and $1p$ removal reactions and with γ-ray multiplicities $M_\gamma < 4$. Single transitions were observed at 915(12) keV for ^{27}F keV and at 1080(18) keV for ^{29}F, and assigned to $1/2^+_1 \rightarrow 5/2^+_{\text{g.s.}}$ decays due to their agreement with

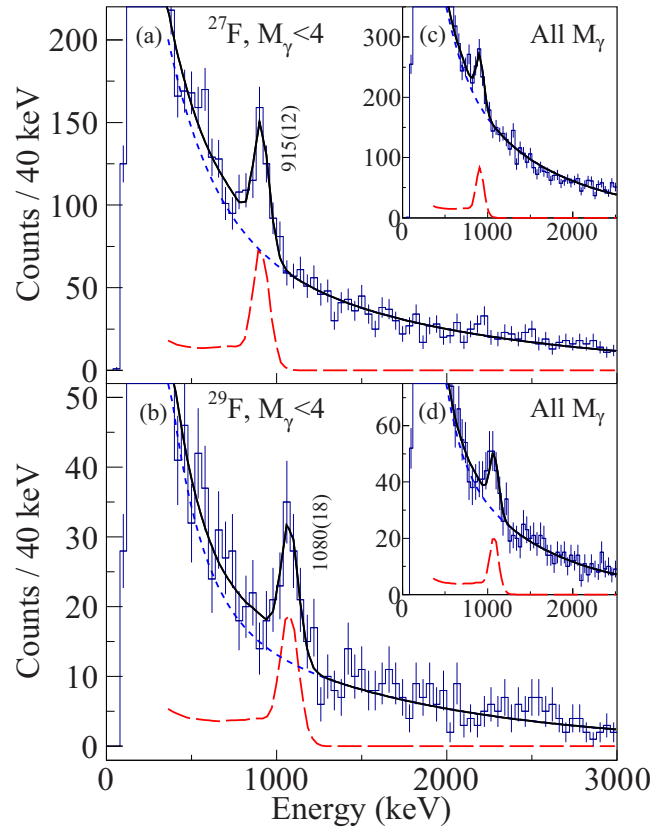

FIG. 2. Doppler-corrected γ-ray spectra with the condition $M_\gamma < 4$ in coincidence with ^{27}F [upper panel (a)] and ^{29}F [lower panel (b)] reaction residues from the ^{30}Ne secondary beam. The black solid lines show the sum of fitted experimental exponential background (blue dotted) and simulated, Doppler-shift corrected DALI2 response functions (red dotted) for transition energies of 915 and 1080 keV, respectively. Conditions on M_γ were removed for the insets (c) and (d).

shell model calculations discussed below. Note that populated negative-parity states in ^{29}F would require the removal of p-shell protons and likely lie at high excitation energies due to the large $Z = 8$ shell gap. Further support for the spin assignment in ^{29}F is given by an excited-state population of only 11(3)%, which can be understood by primarily $0d_{5/2}$ protons removed from ^{30}Ne in the reaction. Absolute cross sections are discussed in Ref. [37] together with the $1n$ removal reaction from ^{30}Ne [38]. Restrictions on M_γ were utilized to enhance the peak to total of observed γ-ray transitions, as demonstrated in earlier studies [25,39]. Here, M_γ was defined as the number of observed γ rays within a time window of 30 ns and above the detection threshold of ≈150 keV. Events were combined when the γ rays were detected within a maximum of 200 mm from the central point of the DALI2 crystals involved. The insets in Fig. 2 show spectra with no condition on M_γ for both nuclei, featuring no apparent other excited states. Events with $M_\gamma > 3$ did not contribute significantly to the observed transitions.

GEANT4 simulations were performed to confirm the absence of the reported transitions in Ref. [32] for ^{27}F in the present $1p2n$ removal reaction. The simulations included the intrinsic energy resolution of the DALI2 detectors as well as the secondary beam and reaction products' energy loss and spatial distributions. Free parameters in the fit of the ^{27}F spectrum were the intensities of three simulated γ-ray transitions at 504, 777, and 915 keV and the exponential background. The fit yielded a sizable component only for the transition at 915(12) keV. Similarly, the spectrum of ^{29}F was compared to simulations. Both fit curves are overlaid to the experimental spectra in Fig. 2 and show good agreement with the lineshape of the observed γ-ray transitions.

The assumption of normal filling for ^{27,29}F puts the last proton and neutron inside the sd shell $(0d_{5/2}, 1s_{1/2}, 0d_{3/2})$. Comparisons with shell model calculations restricted to this model space, the USDA/USDB effective interactions [40], and an interaction that includes the higher-lying neutron $0f_{7/2}$ and $1p_{3/2}$ shells, for instance the SDPF-M effective interaction [41,42], can clarify the involvement of intruder components across the $N = 20$ shell gap. The calculations, compared in Fig. 3 with the experimental results, were carried out with the computer code KSHELL [43] for USDA/USDB and with MSHELL64 [44] for SDPF-M. All calculations point to $5/2^+$ ground states and $1/2^+$ first excited states for ^{27,29}F. Of paramount importance are, however, the differences found for the $1/2^+_1$ excitation energies. For USDA/USDB, the respective $1/2^+$ states are located at 1.422 and 1.785 MeV for ^{27}F, already in excess of the experimental findings. More significantly, the $1/2^+$ states of 3.673 and 3.502 MeV for ^{29}F lie more than 2 MeV higher than the observed energy. Contrariwise, with SDPF-M the $1/2^+_1$ levels are located at 1.183 and 0.786 MeV for ^{27}F and ^{29}F, respectively, consistent with the experiment for both nuclei. It is worth mentioning that a similar excitation energy of 0.91 MeV has been calculated for ^{29}F with SDPF-U-MIX, an effective interaction that allows for neutron excitations across the $N = 20$ shell as well [21].

In order to assess the present energy findings and illustrate the connection between the $1/2^+_1$ excitation energy in ^{29}F and the $N = 20$ shell quenching, a closer inspection of nuclear

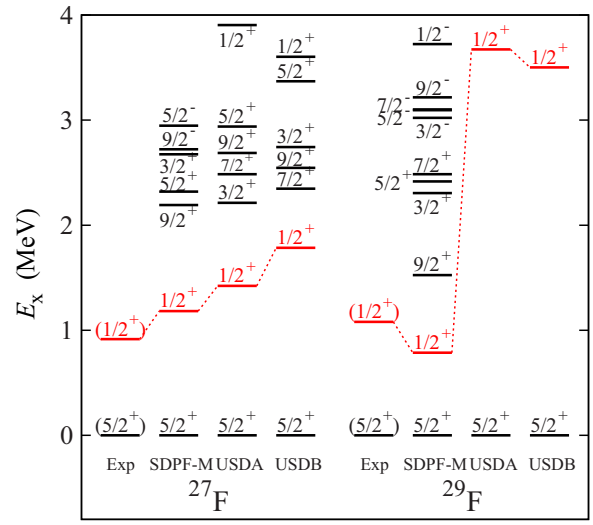

FIG. 3. Experimental energy levels of ^{27,29}F compared with shell model calculations using the USDA/USDB and SDPF-M effective interactions. Only SDPF-M provides an adequate description of the first excited state in ^{29}F. Dashed lines are drawn to guide the eye.

properties in the vicinity is necessary. As pointed out in Fig. 5 of Ref. [41], the neutron effective single-particle energy (ESPE) gap between $0d_{3/2}$ and $0f_{7/2}1p_{3/2}$, calculated with the monopole part of the SDPF-M interaction, decreases as a function of proton number from ^{40}Ca to ^{28}O. Numerically, the neutron ESPE evolve from $0d_{3/2} = -0.968, 0f_{7/2} = 1.681$, and $1p_{3/2} = 1.484$ MeV for ^{29}F to $0d_{3/2} = 0.640, 0f_{7/2} = 2.763$, and $1p_{3/2} = 2.141$ MeV for ^{28}O, resulting in $N = 20$ gaps of 2.452 and 1.501 MeV. Besides excitation energy values, ground-state binding energies, BE, and the $0p0h$ configuration probabilities of having no neutron excitation across the $N = 20$ shell for a given state are of interest to describe the structure of ^{29}F and ^{28}O.

Previous calculations of two neutron-separation energies S_{2n} with SDPF-M have shown excellent agreement with experimental data for $N = 20$ isotones down to ^{30}Ne [20], while USDA/USDB cannot reproduce the BE of island of inversion nuclei (Fig. 10 of Ref. [40]). For the fluorine isotopes $^{19-26}$F, calculated mean BE differences to the atomic mass evaluation AME2012 [45] are 0.220, 0.183, and 0.330 MeV for USDA/USDB, and SDPF-M, respectively. Available experimental data for ^{27,29}F from Refs. [31,46] are presented in Table I together with shell model results. The two mass measurements for ^{27}F differ by about 0.8 MeV, or 4 standard deviations, and shell model values are closer to Ref. [46]. Despite this difference, experimental one-neutron separation energies and calculated excitation energies suggest that only one bound excited state exists for ^{27}F, as observed in the experiment.

Adding two neutrons to ^{27}F must bring the $1/2^+_1$ state below S_{2n} in order for it to decay by γ-ray emission. This is confirmed by the measured value of $S_{2n} = 1.443(436)$ MeV [31]. In contrast, only the calculation with SDPF-M provides sufficient additional binding energy ($S_{2n} = 1.028$ MeV), indicating that contributions from neutron orbits above $N = 20$ play an important role in the ground-state configuration of ^{29}F. Enlarging

TABLE I. Comparison between calculated binding and one- and two-neutron separation energies (BE, S_n, S_{2n}) with experimental values from Refs. [31,46] for ^{27,29}F. Energies are given in MeV.

	Nucleus	BE	S_n	S_{2n}
USDA	^{27}F	186.425	1.629	2.745
USDB		186.419	2.034	2.713
SDPF-M		186.215	2.662	2.978
Ref. [46]		186.255(190)	2.107(205)	2.880(204)
Ref. [31]		185.434(260)	1.287(271)	2.060(271)
USDA	^{29}F	186.710	0.816	0.285
USDB		186.402	0.801	−0.017
SDPF-M		187.244	1.614	1.028
Ref. [31]		186.877(350)	1.663(439)	1.443(436)

the ESPE gap by $\Delta_{gap} = 0.5$ MeV increases the $1/2^+$ excitation energy to 0.996 MeV and lowers S_{2n} to 0.307 MeV, which is at variance with the experimental observation. A further increase of the ESPE gap to $\Delta_{gap} = 1.0$ MeV leads to an unbound ^{29}F and an increase of the $1/2^+$ state leads to 1.325 MeV. Figure 4 depicts their evolution up to $\Delta_{gap} = 3.5$ MeV. With increasing ESPE gap, the $1/2^+_1$ energy converges at about 3.4 MeV and thus reaches similar values as USDA/USDB. In addition, calculations were performed for the 2^+_1 and 3^-_1 energy in ^{28}O as a function of the ESPE gap. The former are also shown in Fig. 4 and indicate a strong correlation to the $1/2^+_1$ state in ^{29}F, ranging from 2.122 to 6.910 MeV. A weaker relationship was found for the 3^-_1 state, which varied between 3.317 and 5.042 MeV in the calculated interval of Δ_{gap}.

Further analogies between both nuclei are manifested in their wave-function composition as function of Δ_{gap}. Their evolution of $0p0h$ probabilities for ground and first excited $1/2^+_1$ and 2^+_1 states is displayed in the lower panel of Fig. 4. With the original SDPF-M interaction, ground and first excited state $0p0h$ probabilities of 7.9% and 1.0% are calculated for ^{29}F. These probabilities are similar to the corresponding values of 10.9% and 0.0% for ^{28}O. When enlarging Δ_{gap}, similar values for the ground-state configurations are obtained, which gradually converge to a normal filling. On the other hand, the configuration for the $1/2^+_1$ state in ^{29}F diverges very slowly from the 2^+_1 configuration of ^{28}O. The latter can be formed only by neutron excitation across the $N = 20$ shell gap within the given model space and must therefore remain zero. These commonalities are supported by an inspection of the calculated spectroscopic factors of a proton added to ^{28}O. Dominant configurations are $5/2^+_{g.s.}$: $^{28}\mathrm{O}(0^+_{g.s.}) \otimes 0d_{5/2}$ and $1/2^+_1$: $^{28}\mathrm{O}(2^+_1) \otimes 0d_{5/2}$, once again revealing a firm connection between the respective ground and excited states.

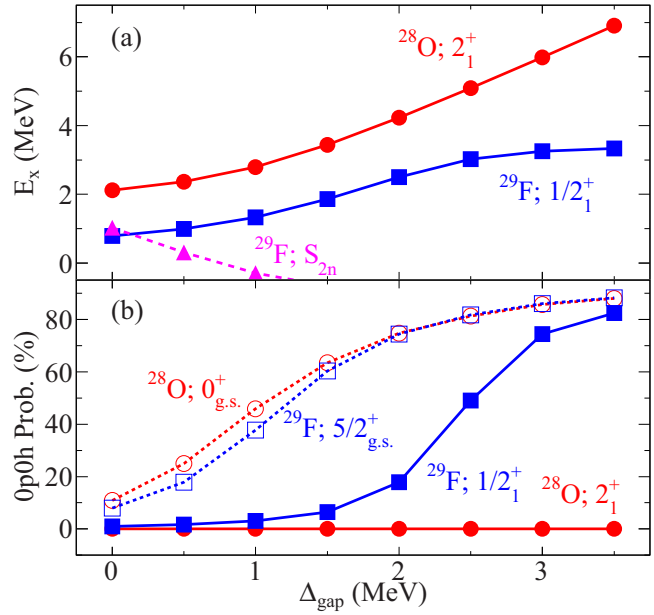

FIG. 4. Correlation between first excited states [top panel (a)] and $0p0h$ wave-function compositions of ground and first excited state [bottom panel (b)] for ^{29}F and ^{28}O as function of a varied $N = 20$ gap with the SDPF-M interaction. Calculated two-neutron separation energies for ^{29}F are also shown. Original SDPF-M values correspond to $\Delta_{gap} = 0$.

In summary, two new excited states were observed in ^{27,29}F and both were assigned spins and parities of $1/2^+_1$. Experimental and calculated neutron separation energies indicate that these are the only bound excited states of the two nuclei. Neutron orbits beyond the $N = 20$ shell are necessary for a correct description of ^{29}F, suggesting a persistent shell quenching towards ^{28}O. In view of the large analogies, the $1/2^+_1$ state of ^{29}F can be regarded as bound representation of the 2^+_1 state of ^{28}O and used for a first indication of its excitation energy. Calculations with the SDPF-M interaction yield a BE of 166.86 MeV and suggest that the location of the 2^+_1 state lies below 3 MeV. Its unbound excitation energy might, however, be largely influenced by continuum effects and three nucleon forces, as evidenced already by the recently observed 2^+_1 energy of ^{26}O [47].

We would like to express our gratitude to the RIKEN Nishina Center accelerator department for providing a stable and high intensity ^{48}Ca primary beam and thank the BigRIPS team for their efforts in preparing the secondary beams.

[1] O. Haxel, J. Jensen, and H. Suess, Phys. Rev. **75**, 1766 (1949).
[2] M. Goeppert Mayer, Phys. Rev. **75**, 1969 (1949).
[3] O. Sorlin and M.-G. Porque, Prog. Part. Nucl. Phys. **61**, 602 (2008).
[4] A. Huck, G. Klotz, A. Knipper, C. Miehe, C. Richard-Serre, G. Walter, A. Poves, H. L. Ravn, and G. Marguier, Phys. Rev. C **31**, 2226 (1985).
[5] C. Hoffman *et al.*, Phys. Lett. B **672**, 17 (2009).
[6] D. Steppenbeck *et al.*, Nature (London) **502**, 207 (2013).
[7] F. Wienholtz *et al.*, Nature (London) **498**, 346 (2013).
[8] J. Fujita and H. Miyazawa, Prog. Theor. Phys. **17**, 360 (1957).
[9] T. Otsuka, R. Fujimoto, Y. Utsuno, B. A. Brown, M. Honma, and T. Mizusaki, Phys. Rev. Lett. **87**, 082502 (2001).

[10] T. Otsuka, T. Suzuki, R. Fujimoto, H. Grawe, and Y. Akaishi, Phys. Rev. Lett. **95**, 232502 (2005).
[11] T. Otsuka, T. Suzuki, M. Honma, Y. Utsuno, N. Tsunoda, K. Tsukiyama, and M. Hjorth-Jensen, Phys. Rev. Lett. **104**, 012501 (2010).
[12] G. Hagen, M. Hjorth-Jensen, G. R. Jansen, R. Machleidt, and T. Papenbrock, Phys. Rev. Lett. **108**, 242501 (2012).
[13] J. D. Holt, J. Menendez, and A. Schwenk, Eur. Phys. J. A **49**, 39 (2013).
[14] S. K. Bogner, H. Hergert, J. D. Holt, A. Schwenk, S. Binder, A. Calci, J. Langhammer, and R. Roth, Phys. Rev. Lett. **113**, 142501 (2014).
[15] R. Kanungo *et al.*, Phys. Rev. Lett. **102**, 152501 (2009).
[16] O. Tarasov *et al.*, Phys. Lett. B **409**, 64 (1997).
[17] H. Sakurai *et al.*, Phys. Lett. B **448**, 180 (1999).
[18] C. Détraz, D. Guillemaud, G. Huber, R. Klapisch, M. Langevin, F. Naulin, C. Thibault, L. C. Carraz, and F. Touchard, Phys. Rev. C **19**, 164 (1979).
[19] T. Motobayashi *et al.*, Phys. Lett. B **346**, 9 (1995).
[20] Y. Utsuno, T. Otsuka, T. Mizusaki, and M. Honma, Phys. Rev. C **64**, 011301(R) (2001).
[21] E. Caurier, F. Nowacki, and A. Poves, Phys. Rev. C **90**, 014302 (2014).
[22] E. K. Warburton, J. A. Becker, and B. A. Brown, Phys. Rev. C **41**, 1147 (1990).
[23] K. Yoneda *et al.*, Phys. Lett. B **499**, 233 (2001).
[24] A. Gade *et al.*, Phys. Rev. Lett. **99**, 072502 (2007).
[25] P. Doornenbal *et al.*, Phys. Rev. Lett. **111**, 212502 (2013).
[26] Y. Yanagisawa *et al.*, Phys. Lett. B **566**, 84 (2003).
[27] P. Doornenbal *et al.*, Phys. Rev. Lett. **103**, 032501 (2009).
[28] P. Doornenbal *et al.*, Prog. Theor. Exp. Phys. **2014**, 053D01 (2014).
[29] A. Poves and J. Retamosa, Phys. Lett. B **184**, 311 (1987).
[30] G. Christian *et al.*, Phys. Rev. Lett. **108**, 032501 (2012).
[31] L. Gaudefroy *et al.*, Phys. Rev. Lett. **109**, 202503 (2012).
[32] Z. Elekes *et al.*, Phys. Lett. B **599**, 17 (2004).
[33] T. Kubo *et al.*, Prog. Theor. Exp. Phys. **2012**, 03C003 (2012).
[34] N. Fukuda, T. Kubo, T. Ohnishi, N. Inabe, H. Takeda, D. Kameda, and H. Suzuki, Nucl. Instr. Meth. B **317**, 323 (2013).
[35] S. Takeuchi, T. Motobayashi, Y. Togano, M. Matsushita, N. Aoi, K. Demichi, H. Hasegawa, and H. Murakami, Nucl. Instr. Meth. A **763**, 596 (2014).
[36] S. Agostinelli *et al.*, Nucl. Instr. Meth. A **506**, 250 (2003).
[37] J. Lee *et al.*, Prog. Theor. Exp. Phys. **2016**, 083D01 (2016).
[38] H. Liu *et al.*, Phys. Lett. B **767**, 58 (2017).
[39] H. Wang *et al.*, Phys. Rev. C **88**, 054318 (2013).
[40] B. A. Brown and W. A. Richter, Phys. Rev. C **74**, 034315 (2006).
[41] Y. Utsuno, T. Otsuka, T. Mizusaki, and M. Honma, Phys. Rev. C **60**, 054315 (1999).
[42] Y. Utsuno, T. Otsuka, T. Glasmacher, T. Mizusaki, and M. Honma, Phys. Rev. C **70**, 044307 (2004).
[43] N. Shimizu, arXiv:1310.5431 [nucl-th] (unpublished).
[44] T. Mizusaki, N. Shimizu, Y. Utsuno, and M. Honma, Computer code MSHELLX64 (unpublished).
[45] G. Audi, M. Wang, A. Wapstra, F. Kondev, M. MacCormick, X. Xu, and B. Pfeiffer, Chin. Phys. C **36**, 1287 (2012).
[46] B. Jurado *et al.*, Phys. Lett. B **649**, 43 (2007).
[47] Y. Kondo *et al.*, Phys. Rev. Lett. **116**, 102503 (2016).